Time-resolved-photoluminescence spectra of MnO and MnS

1994 J. Phys.: Condens. Matter 6 7317

(http://iopscience.iop.org/0953-8984/6/36/014)

J. Phys.: Condens. Matter 6 (1994) 7317–7327. Printed in the UK

Time-resolved-photoluminescence spectra of MnO and MnS

Bernard Piriou†, Jeannette Dexpert-Ghys† and Shōsuke Mochizuki‡

† Laboratoire PCM, ERS 070/CNRS, Ecole Centrale Paris, F-92295 Chatenay Malabry Cédex, France

‡ Department of Physics, College of Humanities and Sciences, Nihon University 3-25-40 Sakurajosui, Setagaya-ku, Tokyo 156, Japan

Received 12 April 1994

Abstract. We have studied the time evolution of the photoluminescence spectra of MnO and MnS at different temperatures. In MnO crystals, of the two emission bands A and B, the broad band A observed at the high-energy side under steady-state measurement conditions consists of two broad bands A′ and A″ differing in their transient properties. A′ is the fastest-decaying band. Each band A′ and A″ is accompanied at low temperature by a set of narrow sidebands. The emitting levels of the A′ and A″ bands are thermally depopulated via a level lying about 130 cm^{-1} higher. The A′ and A″ emissions are assigned to Mn ions unperturbed and perturbed by impurities, respectively. The broad band B observed on the low-energy side grows to the detriment of emission A′ and A″ with increasing temperature. It is tentatively assigned to Mn^{2+} perturbed by Mn ions with higher valence. The results on MnS powder show similarities with those of MnO, but they are affected by some surface effects.

1. Introduction

Since 1990, we have reported the spin-wave-assisted-photoluminescence spectra in the simplest antiferromagnetic compounds, MnO (Mochizuki *et al* 1990, 1992) and MnS (Mochizuki 1990, Mochizuki and Takayama 1991). It was found that the photoluminescence spectra measured at nearly-steady-state conditions and their temperature dependences are very similar. In both compounds, the spectra consist of two emission bands, the A band (MnO, 1.71 eV; MnS, 1.64 eV; at 40 K) and the B band (MnO, 1.25 eV; MnS, 1.44 eV; at 40 K), with large Stokes shifts and with respect to the absorption-band maxima (0.37 eV at 77 K for MnO and 0.43 eV for MnS in the range 5–40 K). At low temperatures, only the A band is observed and, with increasing temperature, the B band begins to grow at the expense of the A band. However, surprisingly enough, some of the as-grown crystals of MnO show only the B-band emission at 77 K. The A band in MnO and MnS is assigned to the $^4T_{1g}$–$^6A_{1g}$ transition of Mn^{2+} ions. The complete disappearance of the A band at the Néel temperature and the drop in the B-band intensity prove that they are closely related to the magnetic ordering of Mn^{2+} spins.

In the present paper new experimental data, i.e. low-temperature photoluminescence measured with time resolution on MnO and MnS will be described. Some of these observations are in good agreement with previously reported results on concentrated Mn^{2+} antiferromagnets. In contrast other observations do not fit the models generally accepted in the literature.

0953-8984/94/367317+11$19.50

2. Experimental details

The MnO single crystals used in the present experiments were one as-grown crystal that showed the one-band-type emission, and one crystal annealed in a 10% H_2–90% Ar atmosphere at 1273 K; such annealing yields fully reduced MnO. The MnS specimen used in the present experiments was compacted MnS powder and contains Si (0.009%), Ni (0.003%), Ca (less than 0.001%), Cu (0.001%), Ag (less than 0.001%) and Mg (less than 0.001%).

A dye laser (Jobin–Yvon LA01/E1T) pumped by a pulsed N_2 laser (Jobin–Yvon LA01S) was used as excitation source. The spectra were recorded with the monochromator of a Cary-14 spectrophotometer equipped with a photomultiplier (Hamamatsu R2658). The information was extracted via a digital oscilloscope (Tektronix 2430) coupled to a 16-bit computer (BFM 187). In this set-up, the time evolution of the emission was recorded for each pulse. The emitted intensity was numerically integrated for a chosen gate after a given delay time with respect to the pulse. By programming the data collection as a function of the spectrometer scanning, the time-resolved emission spectra for various integration gates were simultaneously recorded. In order to appreciate the time effect, the spectra will be presented after normalization to maximum value, although their overall intensity decreases as time elapses. The steady-state emission spectra under Ar-ion-laser excitation (488 nm line) and the absorption spectra were calibrated on the same monochromator (Jobin–Yvon H-20 UV).

The spectral response of the optical system, including the focusing lens, was carefully measured using a calibrated quartz–halogen lamp and was used to correct the raw data.

The temperature variation was achieved using an He-gas-flow-type cryostat system (SMC-TBT) in which a Pt resistor and a C resistor (Lakeshore Cryotronics Inc. CGR-1-2000) were used for temperature (T) determination above and below 80 K, respectively.

3. Results

The raw emission spectra $I_r(\lambda)$ were recorded versus wavelength λ at constant slit width. After correction for the spectral response of the apparatus $F(\lambda)$, they were converted to the energy E scale, following $I(E) = (\lambda^2/hc)I_r(\lambda)/F(\lambda)$. As may be seen in the figures hereafter the cut-off of our apparatus (actually that of the photomultiplier) is about 1.3 eV. The shape of the band B on its low-energy side is affected to some extent by the very low sensitivity in this region. Despite this, the observations on the time evolutions of the two bands remain correct.

3.1. MnO

Figure 1 exhibits the spectra at 7 K for the annealed MnO. The emission is made up of a broad asymmetrical band (band A) with narrow high-energy side bands. The decay is nearly exponential with a lifetime of 375 μs and a very weak time-resolution effect appears in the sideband region.

The general trends of the emission when the temperature increases are as follows:

(i) The vanishing of the side-band peaks and the appearance of time evolution within the A band. The band shifts towards lower energies when the observation time increases and also when the temperature increases. These changes occur in the temperature range 30–90 K, that is, in the same range that the shift of the band maximum observed under steady-state excitation (figure 2 of Mochizuki *et al* (1992)).

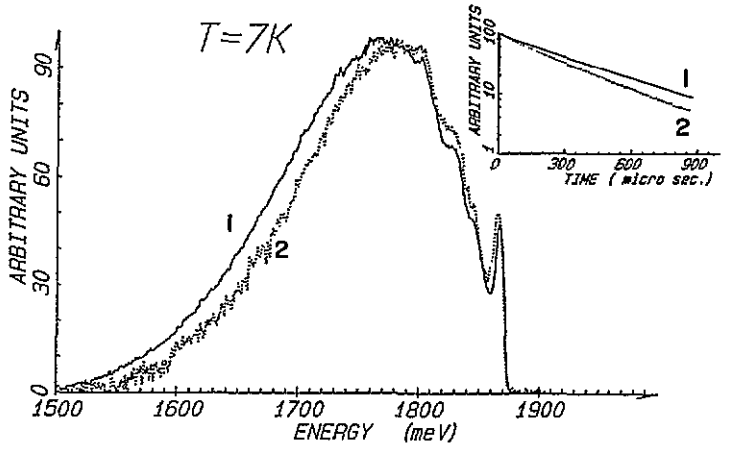

Figure 1. Emission spectra at 7 K in MnO under 21 030 cm^{-1} excitation: full line (1), annealed sample; dotted line (2), as-grown sample. Inset, the corresponding decay curves.

(ii) The relative increase of a second band B: the intensity at peak position of band B becomes superior to that of band A above 80 K.

The time-resolved spectra recorded at 50 K (figure 2) give an example of the evolutions in the temperature range 30–90 K. The shift of the different traces may be understood by considering the decay curves observed near the maximum (1.75 eV, point β on the figure), on the lower-energy side (1.67 eV, α), and on the high-energy side (1.82 eV, γ). At low energy the decay is nearly exponential, whereas the other two curves are markedly non-exponential. The weight of the faster component increases with the monitoring frequency.

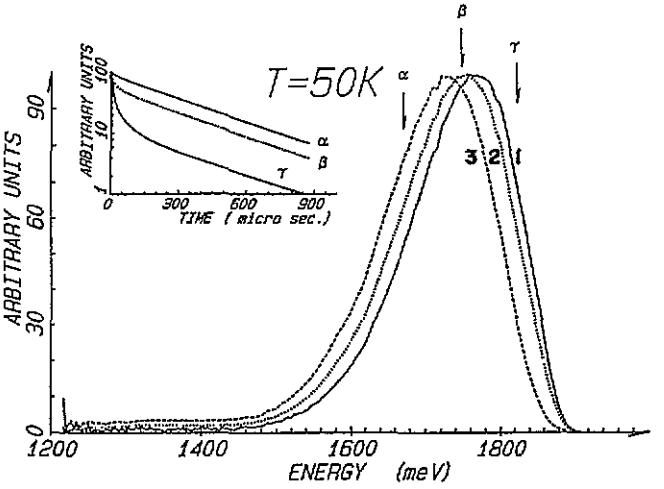

Figure 2. Time-resolved emission spectra at 50 K for annealed MnO under 21 030 cn^{-1} excitation. Delays and gates in microseconds are 1 and 3 (spectrum 1), 4 and 4 (spectrum 2), 15 and 18 (spectrum 3). Inset, decay profiles observed at $\alpha = 1.67$ eV, $\beta = 1.75$ eV and $\gamma = 1.82$ eV.

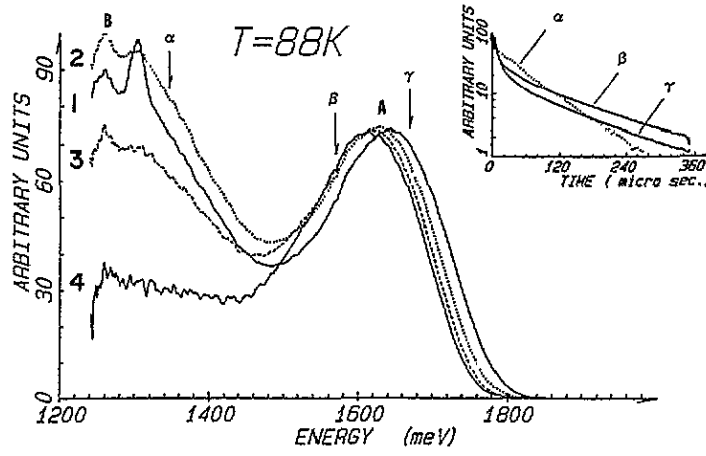

Figure 3. Time-resolved emission spectra at 88 K in the annealed MnO under 21 030 cm^{-1} excitation. Delays and gates in microseconds are 20 and 20 (spectrum 1), 35 and 49 (spectrum 2), 78 and 89 (spectrum 3), 156 and 156 (spectrum 4). Inset, decay curves observed at $\alpha = 1.35$ eV, $\beta = 1.576$ eV and $\gamma = 1.675$ eV. The sharp band appearing at about 1.3 eV in spectrum 1 is due to the second-order diffraction of the excitation line.

The traces in figure 3 are the time-resolved spectra at 88 K. The shift of the A band is explained as above by the weight of the fast component on the high-frequency edge. Considering the decay curves shown in the inset, the evolution of the relative intensities is well described. The lifetimes are 67 μs for band B (exponential decay), and 140 μs for the slow component of the A band, but the fast component governs the decay of the A band during the first 10 μs. Two kinds of behaviour are thus observed: in the range 0–120 μs, band A decreases faster than B, whereas at longer times the reverse occurs. These decays cause the 'up and down' evolution of the B-band intensity with respect to band A in the spectra 1–4 in figure 3, each one being normalized at the A-band maximum. Approaching the Néel temperature, the B band becomes prominant with respect to band A.

The observation of the as-grown MnO crystal at 7 K gives similar results: a broad band A, narrow side bands, and very weak time resolution, but the entire emission intensity is greatly reduced with respect to that of the annealed specimens as shown by considering the signal/noise ratios in figure 1. The decay at 7 K is nearly exponential: the lifetime is 290 μs, shorter than that in the heat-treated crystal.

At higher temperature, the observations on the as-grown crystal are qualitatively analogous to those reported for the heat-treated MnO. Besides the shift of the A band, with increasing temperature and with increasing delay after the excitation pulse, the spectra are characterized by the variation in A/B ratio (see figure 4). In this specimen, although the A emission was never seen under steady-state conditions, it is also present but can be detected only at very short delays after the excitation pulse. Simultaneously with the shortened lifetime, the maximum frequency of the A band is higher in the as-grown sample (about 1.70 eV at 85 K versus 1.62 eV in the heat-treated specimen). At a given temperature the A/B intensity ratio is lower in the as-grown than in the annealed sample (see figures 3 and 4).

3.2. MnS

The photoluminescence of MnS polycrystals at low temperature exhibits mainly the A band,

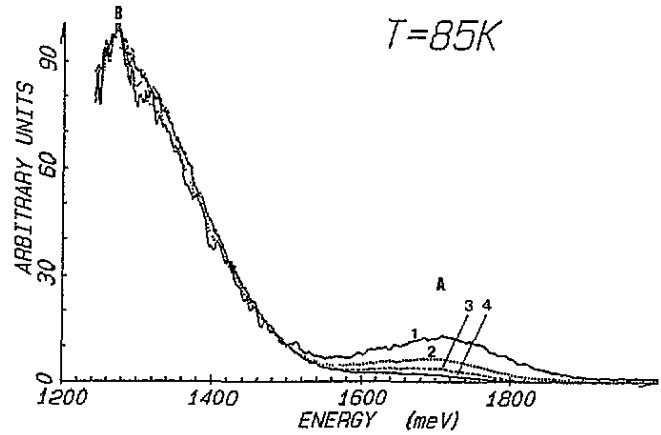

Figure 4. Time-resolved emission spectra at 85 K in the as-grown MnO, showing band A at short delay. The excitation wavenumber is 21 030 cm^{-1}. Delays and gates in microseconds are 1 and 3 (spectrum 1), 4 and 4 (spectrum 2), 8 and 8 (spectrum 3), 16 and 18 (spectrum 4). The spectra are normalized to the maximum of the B band.

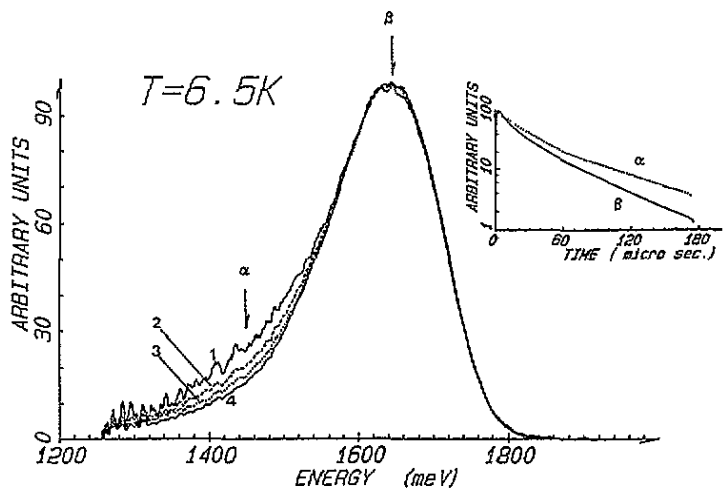

Figure 5. Time-resolved emission spectra at 6.5 K in MnS. Delays and gates in microseconds are 2 and 8 (spectrum 1), 10 and 10 (spectrum 2), 20 and 20 (spectrum 3), 39 and 44 (spectrum 4). Inset, decay curves observed at $\alpha = 1.45$ eV and $\beta = 1.65$ eV.

without any time-resolution effect, except on the lower-energy wing where band B begins to appear at long times after the excitation (see for instance in figure 5 the spectra and decays recorded at 6.5 K). In contrast to the oxide samples, no sidebands are observed, and the decay at peak maximum (β on the figure) is already non-exponential at this low temperature. When the temperature increases the emission characteristics change drastically. Figure 6 for instance displays the spectra observed at 55 K: at 5 μs delay, one sees essentially band A and after 50 μs, essentially B. The A emission remains just detectable below 15 μs at 84 K (see figure 7). At this temperature, time resolution occurs within the B band. It results in the narrowing of the band at longer delays rather than a shift of the whole band.

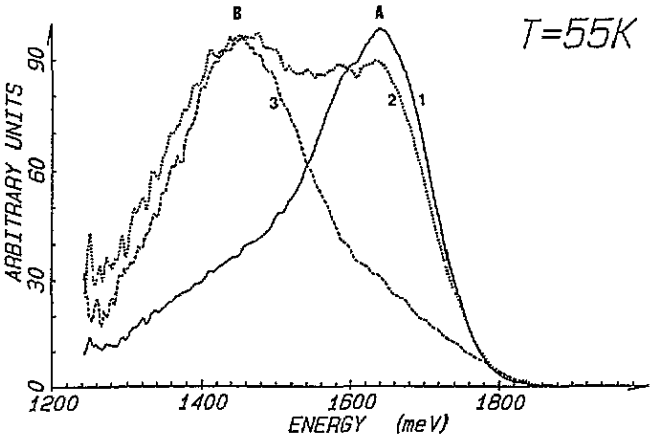

Figure 6. Time-resolved emission spectra at 55 K in MnS. The excitation wavenumber is 21 030 cm^{-1}. Delays and gates in microseconds are 2 and 8 (spectrum 1), 10 and 10 (spectrum 2), 40 and 40 (spectrum 3).

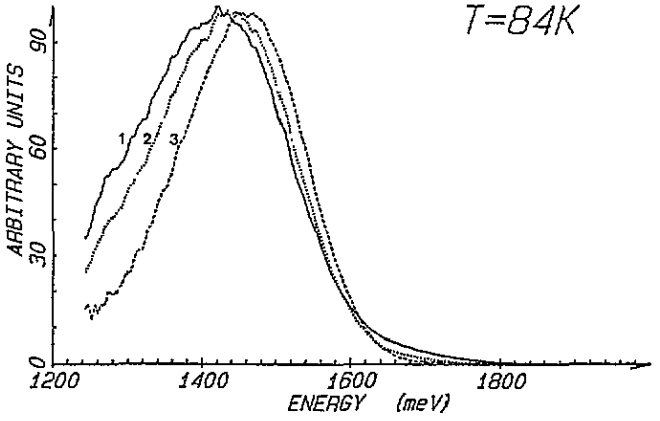

Figure 7. Time-resolved emission spectra at 84 K for MnS, showing the trace of band A at short delay. The excitation wavenumber is 21 030 cm^{-1}. Delays and gates in microseconds are 10 and 10 (spectrum 1), 40 and 40 (spectrum 2), 78 and 156 (spectrum 3).

3.3. The temperature dependence of lifetime in MnO and MnS

As stated above the time dependences of the spectra are very important in MnO, mainly above 30 K. In this subsection will be described the temperature dependence of the emission decays observed at different frequencies in band A and only at the maximum of band B (the decays are the same for all frequencies in this band). The temperature dependences of the lifetimes are reported in figure 8. The decay profiles are fitted by a sum of exponentials. $\tau_{A''}$ is the lifetime measured on the low-energy side of band A, where the decay is approximately single exponential. At first sight (see figures 2 and 3) the decay on the high-energy side of band A is a sum of two exponentials, but a very fast third component with a lifetime of 10 μs was added to improve the fit. The slow component was considered to be $\tau_{A''}$ previously determined and the fast component to be $\tau_{A'}$ was deduced. At low temperature,

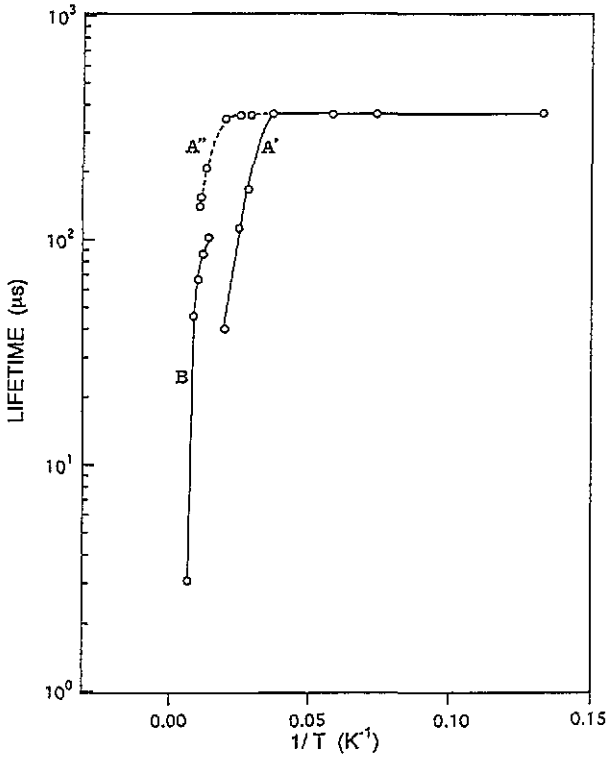

Figure 8. The temperature dependence of the emission lifetimes in the annealed MnO (see the text for the definitions of the lifetimes). Full and broken curves are added between the points as a guide to show the behaviours.

below 30 K, $\tau_{A'}$ and $\tau_{A''}$ cannot be distinguished.

As shown on the curve, $\tau_{A'}$ drastically drops between 30 and 50 K whereas the drop for $\tau_{A''}$ occurs between 50 and 90 K. Two different regimes are thus observed for the A band between 30 and 90 K.

In figure 8 are also plotted the lifetimes of band B between 70 and 140 K in the range where measurements were possible. The decays are single exponentials and the lifetimes vary from 100 to about 3 μs.

The same observations hold qualitatively for the A band in the as-grown and annealed MnO. The B-band decay could actually be recorded between 70 and 140 K. The profile is exponential; the lifetime varies from 90 μs at 70 K to 45 μs at 100 K, then falls to 3 μs at 140 K.

The time and temperature dependences in MnS are very different from those in the oxide samples. The A-band decay is non-exponential even at the lower temperature investigated (6.5 K); it may be decomposed in two exponential parts with $\tau_1 = 45$ μs and $\tau_2 = 12$ μs. There is no change in the decays up to 25 K. At this temperature the B emission begins to grow and overlaps the A emission, influencing the observed decays by introducing a slower third component with $\tau_3 = 71$ μs. The influence of the B emission increases with increasing temperature but the faster of the two decay components proper to band A may be followed from 12 μs at 35 K to 1.7 μs at 70 K. Above this temperature the A band is no longer detected. The luminescence decay measured on the maximum of the B band is

moreover composed of two exponentials, τ_3 (71 μs) and τ_4 (17 μs). These values do not change between 35 and 75 K; both decrease above this temperature, reaching respectively 14 and 4 μs at 137 K, the upper limit investigated.

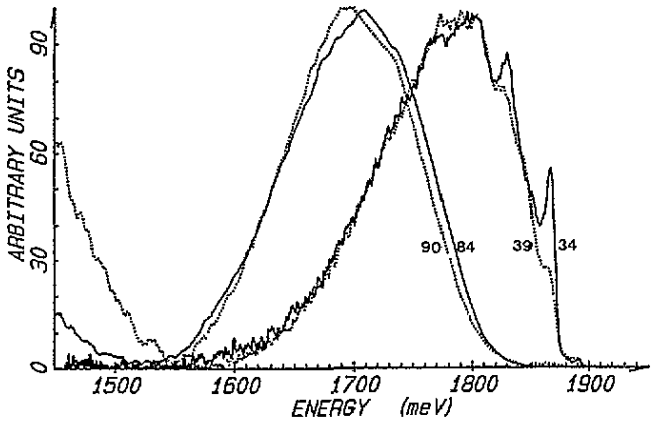

Figure 9. The fast contribution (A′ emission) to the spectra of annealed MnO calculated at four temperatures. These spectra are the computed difference (long-delay emission after pulse − short-delay emission after pulse). The numbers beside the spectra indicate the temperature (in kelvin) of the specimen.

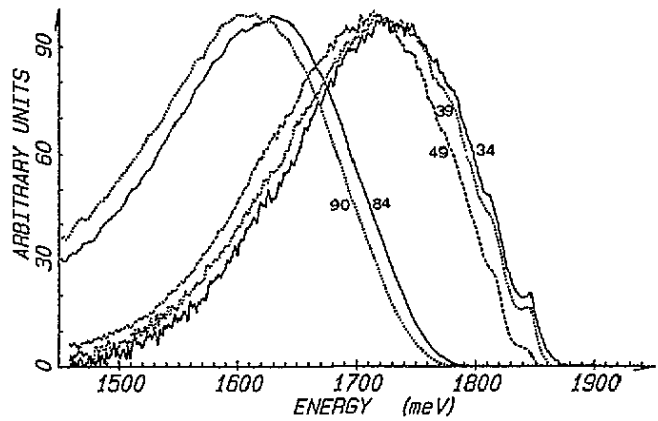

Figure 10. The slow contribution (A″ emission) to the spectra of annealed MnO calculated at five temperatures. These spectra are the computed difference (long-delay emission after pulse − short-delay emission after pulse). The numbers beside the spectra indicate the temperature (in kelvin) of the specimen.

4. Discussion

First the photoluminescence of MnO will be discussed. Having observed a complex time evolution within band A in the range 30–90 K, we have tried to put forward variations

in the spectral distribution that could be related to emissions with different lifetimes. At a given temperature, the calculated difference spectra (short-delay emission − long-delay emission) and reciprocally long delay − short delay give an image of the 'pure' short-time (and reciprocally long-time) emission spectra. For the subtraction of one of the spectra from the other, adequate weighting factors were used in order to eliminate any negative part in the computed difference spectra. The results of these calculations at different temperatures are shown in figures 9 and 10. Below 25 K and in the 55–80 K temperature range the time-resolution effect is not sufficient to obtain correct difference spectra. Considering the widths of the sidebands, their wavenumbers are estimated with 5 cm^{-1} accuracy. One can identify the short-time A′ emission made up essentially of the narrow sidebands denoted a (15 051 cm^{-1}, 1.866 eV), c (14 756 cm^{-1}, 1.829 eV) and d (14 539 cm^{-1}, 1.802 eV) at 39 K, which decrease in intensity as the temperature rises, keeping the same energy, and leave an unresolved band that shifts towards lower energies when the temperature increases. For the long-time emission A″ one identifies two narrow side bands b (14 893 cm^{-1}, 1.846 eV) and x (14 647 cm^{-1}, 1.815 eV) on a broader component that shifts strongly towards lower energies with increasing temperature, whereas the sidebands decrease in intensity, still peaking at the same energies. It is worth pointing out that actually two groups of narrow bands are differentiated with respect to their time evolution. The multicomponent character of the broad Mn^{2+} emission has already been observed in other compounds. Kambli *et al* (1984) pointed out for Rb_2MnCl_4 and $Rb_3Mn_2Cl_7$ that at least two components with different decay times are present in the A emission. For the former compound Tsuboi *et al* (1992) have specified the temperature dependence of the lifetimes of two components.

In a preceding paper (Mochizuki *et al* 1992) the emission sidebands (a, b, c, and d) observed under steady-state conditions have been assigned. The attribution was based on the mirror relation existing between the emission and absorption data (Yokogawa *et al* 1977). The sidebands a, c and d may be assigned as exciton–magnon, exciton–magnon–TO-phonon and exciton–magnon–LO-phonon combinations of an exciton line (not seen). On the fast-emission spectra calculated between 34 and 49 K (figure 9) a weak line (a′) also appears at 15 251 cm^{-1} (1.890 eV). This is not seen at temperatures below 30 K and is interpreted as anti-Stokes emission of the exciton–magnon combination. The energy gap between a′ and a is 200 ± 10 cm^{-1}, in reasonable agreement with twice the 112 cm^{-1} found for the peak in the magnon density of states (Motizuki and Harada 1970). Considering these emission data, the pure exciton line is expected at $15\,151 \pm 5$ cm^{-1} (1.878 eV). After the previous work of Yokogawa *et al* (1977) the frequency of the exciton line measured in the absorption is 15 532 cm^{-1}. Considering this discrepancy we have recorded the absorption and emission spectra on the same spectrometer calibrated with the 15 533 cm^{-1} line of a Cd discharge lamp. The energy found for the a sideband in absorption was 15 656 cm^{-1} (1.941 eV), in rather good agreement with Yokogawa's results. This observation locates the pure exciton line between 15 556 and 15 544 cm^{-1}, depending on the value taken for the magnon energy (100 or 112 cm^{-1}). The two spectra (emission and absorption) never overlap, contrarily to what has been observed in other Mn compounds (i.e. MnF_2 (Greene *et al* 1968), $CsMnF_3$ (Moncorge *et al* 1982), $BaMnF_4$ (Moncorge *et al* 1984), Rb_2MnCl_4 and $Rb_3Mn_2Cl_7$ (Kambli *et al* 1984). For MnO there is a shift of 390 ± 10 cm^{-1} between the more accurate estimation of the absorption and emission exciton lines. The observed energy gap and mirror relation indicate together that there is some self-trapping of the excitons in MnO.

The long-lifetime group contains sidebands b and x; the former appears more clearly after the difference (long- − short-delay) spectrum has been calculated. The x sideband is revealed by the difference and was not observed in steady-state measurements. One can

assign b and x to sidebands of an exciton line associated with an impurity. As seen in figures 9 and 10 the sidebands are better resolved in the short-time emission A′ (figure 9) than in the long-time one, A″ (figure 10). This is another argument in favour of an impurity-associated emission for A″ since in this case the spin selection rules for emission will be relaxed. The b sideband is thought to be magnon assisted and x magnon + TO phonon assisted. As for the short-lifetime group, the pure exciton line was not observed.

The variation of τ_A, versus T (shown in figure 8) follows the exponential gap law:

$$1/\tau = 1/\tau_0 + C\exp(-\Delta E/kT) \tag{1}$$

in which τ_0 is the low-temperature lifetime. C may be considered as the probability of deexcitation by thermal activation at high temperatures and ΔE is the activation energy of the process. The parameters found for the band A′ are $\tau_0 = 370\ \mu s$ ($1/\tau_0 = 2.7 \times 10^3\ s^{-1}$), $C = 5.7 \times 10^6\ s^{-1}$ and $\Delta E \sim 130\ cm^{-1}$. The deexcitation by a non-radiative process for band A′ occurs via an upper level or a potential barrier lying 130 cm^{-1} above the exciton line at 15 151 cm^{-1}.

The lifetimes of Mn^{2+} emission have been reported for several concentrated Mn systems: MnF_2 (Holloway *et al* 1965, Greene *et al* 1968), alkali Mn trifluorides (Holloway *et al* 1965, Moncorge *et al* 1982) and $RbMnCl_4$ (Tsuboi *et al* 1992). The lifetimes at low temperature in these compounds (up to 60 ms in $RbMnF_3$) are much higher than our data on MnO. The temperature dependences of the lifetimes measured in these works follow the law (1). The activation energy is generally interpreted as the difference between the first excited energy level of the unperturbed Mn^{2+} ions and the levels of localized traps (impurity-perturbed Mn^{2+} ions). Such a model is convenient to explain the fast energy transfer by the unlocalized free-exciton state. In the case of MnO, the value of the activation energy is 130 cm^{-1}, far from the 390 cm^{-1} estimated for an impurity-induced scheme. On the contrary this value is close to the maximum of the one-magnon density of states (Motizuki and Harada 1970). A very similar observation has been reported in the case of Rb_2MnCl_4 by Tsuboi *et al* (1992) where the thermal activation energy for the intrinsic emission (37 cm^{-1}) is that of the first phonon sideband. By comparison we then think that the A′ emission is related to unperturbed Mn^{2+} ions.

The lifetime of band A″ seems to follow the law (1) but the drop occurs at a higher temperature (above 50 K) than that of A′. The fast decrease of $\tau_{A''}$ could be measured only on a reduced range since the band vanishes above 90 K. The activation energy for A″ in this reduced temperature range seems to be of the same order as that for A′. The components A′ and A″ have the same lifetime at low temperature. The levels A′ and A″ lie at very similar energies, so it may be understood that they have the same transition probability at low temperature when the thermal process does not occur. In addition to the sidebands, A″ emission contains a broad band that shifts towards low energy as the temperature increases. We can assign this contribution to a multiphonon-assisted transition of the exciton line associated with perturbed Mn^{2+}.

As the temperature increases the B band increases to the detriment of bands A′ and A″. One can understand this as some excitation energy transfers from A′ and A″ to B, although no increase of the B band with time was observed on the transient emission curves.

For the as-grown sample at a given temperature, the B/A intensity ratio is greater than that for the annealed sample, which corroborates that band B is associated with the Mn^{2+} ion pertrubed probably by the presence of Mn ions with higher valency in the as-grown sample.

Let us compare the behaviour of MnS with MnO. Already at low temperature (see figure 5) one can take into account an excitation energy transfer from band A to band B

since the B/A emission ratio increases with time elapsed after the excitation pulse. The non-exponential decay of bands A and B at low temperature can be attributed to excitation energy transfer to traps in a disordered structure where the surface effects are important (MnS was a compressed powder sample). Along the same lines the enhancement of the B band (figure 6) with respect to the previous data on MnO can be understood as a relaxation of some selection rule in the energy transfer process. At high temperature (figure 7) the B band presents a biphasic decay; the fast decay component is more important on the low-energy side. This suggests that at least two kinds of perturbed Mn^{2+} ion are present.

5. Summary

We have measured the time-resolved-photluminescence spectra of annealed and as-grown MnO crystals and of MnS powder at various temperatures. The higher-energy band A characterized by the previous investigation of MnO luminescence under the steady-state regime presents a bicomponent character revealed by the time-resolved observation. Two emissions A′ and A″ were distinguished and each emission is characterized by a broad band and a set of narrow sidebands. We suggest that A′ is the emission of unperturbed Mn^{2+} ions and A″ is due to some Mn ions perturbed by impurities as in Mn halides previously described. The results on MnS show similarities with those on MnO, but they are affected by some surface effects.

More detailed study on the non-perturbed and perturbed Mn^{2+} excitons is in progress in order to fully explain the steady-state and time-resolved spectra of MnO and MnS.

Acknowledgments

This study was supported by a grant-in-aid (1991, 1993) for overseas research from Nihon University. We should like to thank Mr Kenji Suzuki (Nihon University) for this assistance in the absorption measurements.

References

Greene R L, Sell D D, Feigelson R S, Imbusch G F and Guggenheim H J 1968 *Phys. Rev.* **171** 600
Holloway W W, Prohosky E W and Kestigian M 1965 *Phys. Rev.* **139** A954
Kambli U, Gudel H U and Briat B 1984 *J. Phys. C: Solid State Phys.* **17** 3113
Mochizuki S 1990 *J. Phys.: Condens. Matter* **2** 7225
Mochizuki S, Piriou B and Dexpert-Ghys J 1990 *J. Phys.: Condens. Matter* **2** 5225
Mochizuki S, Piriou B, Dexpert-Ghys J, Takayama N, Kido G, Mogi I and Suemoto T 1992 *J. Phys.: Condens. Matter* **4** 6501
Mochizuki S and Takayama N 1991 *J. Phys.: Condens. Matter* **3** 2729
Moncorge R, Jacquier B, Madej C, Blanchard M and Brunel L C 1982 *J. Physique* **43** 1267
Moncorge R, Jacquier B, Mahiou R and Uihleim C 1984 *Phys. Rev.* B **30** 997
Motizuki K and Harada I 1970 *Prog. Theor. Phys. Suppl.* **46** 40
Tsuboi T, Silfsten P and Iio K 1992 *Phys. Status Solidi* b **170** K55
Yokogawa M, Taniguchi K and Hamaguchi C 1977 *J. Phys. Soc. Japan* **42** 591